

Effect of Y_2O_3 Nanoparticles on Critical Current Density of $YBa_2Cu_3O_{7-x}$ Thin Films

H. D. Tran^a, D. Sreekantha Reddy^a, C. H. Wie^a, B. Kang^{a,*}, Sangjun Oh^b, Sung-Ik Lee^c

^a Chungbuk National University, Cheongju, Korea

^b National Fusion Research Institute, Daejeon, Korea

^c Sogang University, Seoul, Korea

(Received 17 August 2009; revised or reviewed 23 September 2009; accepted 28 September 2009)

Y_2O_3 나노입자가 $YBa_2Cu_3O_{7-x}$ 박막의 임계전류밀도에 미치는 영향

H. D. Tran^a, D. Sreekantha Reddy^a, 위창환^a, 강병원^{a,*}, 오상준^b, 이성익^c

Abstract

Introduction of proper impurity into $YBa_2Cu_3O_{7-x}$ (YBCO) thin films is an effective way to enhance its flux-pinning properties. We investigate effect of Y_2O_3 nanoparticles on the critical current density J_c of the YBCO thin films. The Y_2O_3 nanoparticles were created perpendicular to the film surface (parallel with the c -axis) either between YBCO and substrate or on top of YBCO, YBCO/ Y_2O_3 /LAO or Y_2O_3 /YBCO/STO, by pulsed laser deposition. The deposition temperature of the YBCO films were varied (780 °C and 800 °C) to modify surface morphology of the YBCO films. Surface morphology characterization revealed that the lower deposition temperature of 780 °C created nano-sized holes on the YBCO film surface which may behave as intrinsic pinning centers, while the higher deposition temperature produced much denser and smoother surface. J_c values of the YBCO films with Y_2O_3 particles were either remained nearly the same or decreased for the samples in which YBCO is grown at 780 °C. On the other hand, J_c values were enhanced for the samples in which YBCO is grown at higher temperature of 800 °C. The difference in the effect of Y_2O_3 can be explained by the fact that the higher deposition temperature of 800 °C reduces intrinsic pinning centers and J_c is enhanced by introduction of artificial pinning centers in the form of Y_2O_3 nanoparticles.

Keywords : YBCO thin film, critical current density, pinning centers, Y_2O_3 nanoparticle

I. Introduction

The discovery of high temperature superconductors (HTS) have opened a new era for the applications of HTS at higher temperatures. For electrical power application purpose, the critical

*Corresponding author.

e-mail: bwkang@chungbuk.ac.kr

current density (J_c) is one of the most important parameters [1].

Many efforts have been devoted to enhance J_c values of YBCO thin films by doping various kinds of impurities into YBCO at nano-scale as artificial pinning centers [2-6]. Requirements for effective artificial pinning centers include size and density of dopants [7]. The size of artificial pinning centers should be in the range of few times of the coherence length of YBCO ($\xi \sim 1.5\text{-}2\text{ nm}$) [8], and the defect density should be equivalent to the order of $(H/2) \times 10^{11}/\text{cm}^2$ [8], where H is the magnitude of the applied magnetic field.

In this work, we investigate the critical current density of the YBCO thin films with introductions of Y_2O_3 nanoparticles. Y_2O_3 was chosen as artificial pinning centers because it is chemically nonreactive with YBCO, and has a simple cubic structure of $a = 1.06\text{ nm}$ [4] with a small lattice mismatch with YBCO, which will allow epitaxial growth of nanoparticles in YBCO matrix. The superconducting properties of YBCO thin films with Y_2O_3 nanoparticles are compared with those of the pure YBCO.

II. Experiment

All of pure YBCO, YBCO thin films with Y_2O_3 nanoparticles were fabricated by using a pulsed laser deposition (PLD) technique. YBCO thin film was deposited at $780\text{ }^\circ\text{C}$ with oxygen pressure of 150 mTorr and laser energy of 250 mJ . Y_2O_3 layer was deposited at $800\text{ }^\circ\text{C}$ with oxygen pressure of 200 mTorr and laser energy of 250 mJ [9, 10].

Two sets of YBCO thin films with Y_2O_3 nanoparticles deposited at different temperatures were prepared: $Y_2O_3(800\text{ }^\circ\text{C})/\text{YBCO}(780\text{ }^\circ\text{C})$ and $Y_2O_3(800\text{ }^\circ\text{C})/\text{YBCO}(800\text{ }^\circ\text{C})$. YBCO and Y_2O_3 layer were deposited on single crystal (100) SrTiO_3 (STO) and (100) LaAlO_3 (LAO) substrates, respectively. Each set consisted of a pure YBCO (YBCO/STO) and YBCO with Y_2O_3 nanoparticles ($Y_2O_3/\text{YBCO}/\text{STO}$ and $\text{YBCO}/Y_2O_3/\text{LAO}$). The

thickness of YBCO layer was 300 nm while Y_2O_3 was deposited as pseudo layer of nanoparticles.

Structural properties of the samples and the existence of impurity phases were characterized by X-ray diffraction (XRD), atomic force microscopy (AFM) measurement [4]. The magnetization curves $M(H)$ were taken by using magnetic property measurement system (MPMS) for the applied field up to 5 T parallel to the c -axis of films.

III. Results and Discussion

First, properties of Y_2O_3 nanoparticles deposited on LAO substrate using 160 laser pulses were analyzed. Figure 1 shows the AFM pictures of Y_2O_3/LAO samples representing a uniform distribution of Y_2O_3 . Mean height and diameter of Y_2O_3 nanoparticles calculated from 2-dimensional (2D) and 3-dimensional (3D) AFM pictures were about 2 nm and 14 nm , respectively.

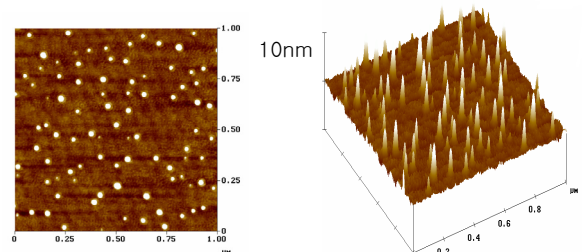


Fig. 1. 2D and 3D AFM pictures of Y_2O_3 nanoparticles deposited on LAO substrate using 160 laser pulses.

XRD patterns of $Y_2O_3(800\text{ }^\circ\text{C})/\text{YBCO}(780\text{ }^\circ\text{C})/\text{STO}$ and pure $\text{YBCO}(780\text{ }^\circ\text{C})/\text{STO}$ samples are shown in Fig. 2. All peaks of YBCO ($00l$) where $l = 2$ to 7 appeared for both samples and the (400) peak of Y_2O_3 in the double layer sample suggest textured growth of both the materials and confirm the existence of Y_2O_3 impurity in the YBCO film.

The second set of samples in which the YBCO layer is deposited at higher temperature of $800\text{ }^\circ\text{C}$ is analyzed by the same procedures. The XRD patterns of $Y_2O_3(800\text{ }^\circ\text{C})/\text{YBCO}(800\text{ }^\circ\text{C})/\text{STO}$ and pure

YBCO(800 °C) samples revealed that all of the peaks of YBCO and Y_2O_3 appear at the same positions with those in Fig. 2. The existence of textured Y_2O_3 impurity on the YBCO film surface at deposition temperature of 800 °C is also confirmed.

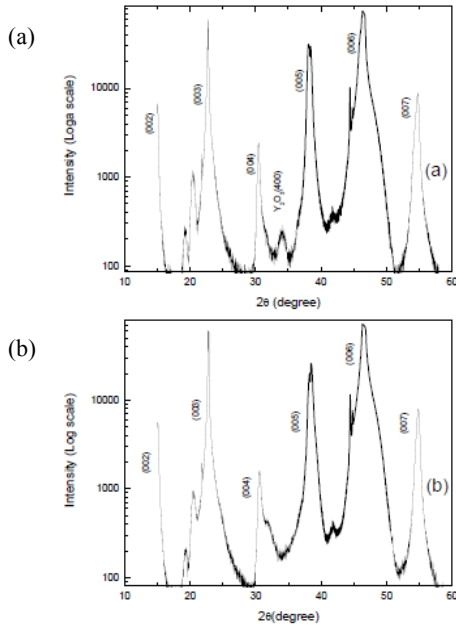


Fig. 2. XRD patterns of (a) $Y_2O_3(800\text{ °C})/YBCO(780\text{ °C})/STO$ and (b) undoped $YBCO(780\text{ °C})/STO$. Appearance of $Y_2O_3(400)$ peak in (a) indicates Y_2O_3 nanoparticles are produced perpendicular to the film surface.

Figure 3(a) and (b) exhibit AFM pictures of the surface morphology of the $Y_2O_3(800\text{ °C})/YBCO(780\text{ °C})/STO$ and $Y_2O_3(800\text{ °C})/YBCO(800\text{ °C})/STO$ samples, respectively. For the YBCO layer deposited at 780 °C, the film surface is not smooth and covered with many deep holes. Properties of the holes are listed in Table 1. Y_2O_3 impurity is coated on top of YBCO in the form of a random distribution of nanoparticles exhibited by the white dots on yellow background. The distribution of Y_2O_3 is not as regular as that of Y_2O_3 on LAO substrate in Fig. 1 due to rough surface of the YBCO layer. For the YBCO deposited at 800°C, the surface of the YBCO layer looks smoother and has smaller number of deep holes than that of the YBCO deposited at 780 °C.

Y_2O_3 nanoparticles are still randomly mounted on the YBCO surface. Properties of the holes are compared with the Y_2O_3 particles in Table 2.

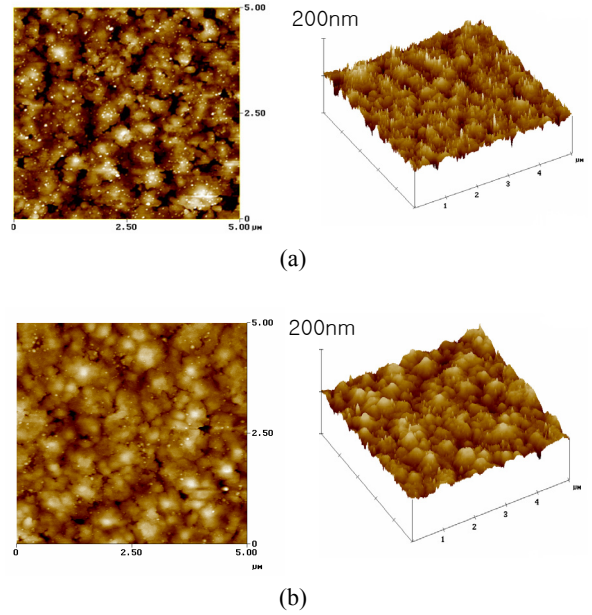


Fig. 3. AFM pictures of (a) $Y_2O_3(800\text{ °C})/YBCO(780\text{ °C})/STO$ and (b) $Y_2O_3(800\text{ °C})/YBCO(800\text{ °C})/STO$ for 160 laser pulses at scale of $5 \times 5\ \mu m^2$.

Table 1. Comparison of Y_2O_3 particles and holes existed on $Y_2O_3(800\text{ °C})/YBCO(780\text{ °C})/STO$ film surface.

	Mean diameter	Mean height (depth)	Density
Y_2O_3	14.0 nm	1.8 nm	$167/\mu m^2$
Holes	30.4 nm	4.6 nm	$78/\mu m^2$

Table 2. Comparison of Y_2O_3 particles and holes existed on $Y_2O_3(800\text{ °C})/YBCO(800\text{ °C})/STO$ film surface.

	Mean diameter	Mean height (depth)	Density
Y_2O_3	14.0 nm	1.8 nm	$167/\mu m^2$
Holes	15.4 nm	2.4 nm	$18/\mu m^2$

Flux pinning properties of the samples were compared by evaluating J_c from the magnetization measurement. Figure 4 represents the field dependence of J_c values of the set of YBCO samples with Y_2O_3

nanoparticles in which the YBCO layer was deposited at 780 °C compared to that of the pure YBCO. The magnetization curves were taken with the magnetic field parallel to the c -axis of the samples. The inset of Fig. 4 shows the magnetization $M(H)$ versus the field H at $T = 5$ K. The critical current density J_c was calculated by using a Bean model, $J_c = 30\Delta M/VR$ [11], where ΔM is the difference of M , V is the sample volume and R is the mean radius of samples which was taken as one fourth of sample length and width. It could be seen that the J_c value of the $Y_2O_3(800\text{ °C})/YBCO(780\text{ °C})/STO$ sample is slightly larger than that of the pure YBCO at zero field and decreases little faster than the pure one as the field is increased. On the other hand, J_c of the $YBCO(780\text{ °C})/Y_2O_3(800\text{ °C})/LAO$ sample decreases much faster than that of the pure YBCO and as a result, the value of J_c became nearly a half of that of the pure at $H = 5$ T. These results suggest two things. First, the Y_2O_3 nanoparticles deposited on top of the YBCO layer do not significantly change pinning property of the sample. It indicates that the Y_2O_3 nanoparticles on top of the YBCO layer do not serve as effective pinning centers. Second, the Y_2O_3 nanoparticles deposited in between the YBCO layer and the substrate drastically degrade pinning property

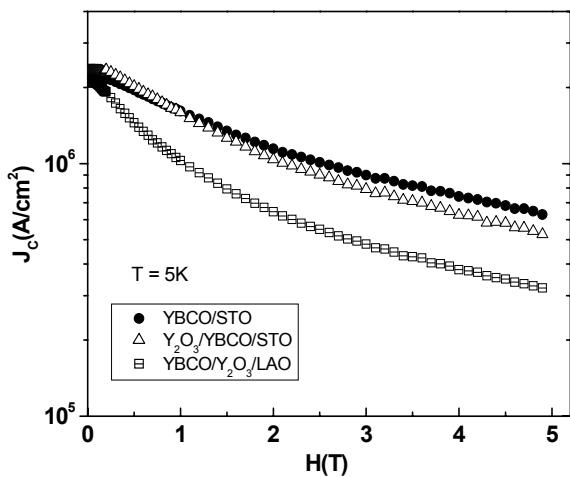


Fig. 4. Comparison of J_c values of YBCO(780 °C)/STO, $Y_2O_3(800\text{ °C})/YBCO(780\text{ °C})/STO$ and YBCO(780 °C)/ $Y_2O_3(800\text{ °C})/LAO$ measured at $T = 5$ K.

of the sample. The reason for this might be not only due to the Y_2O_3 nanoparticles but also due to the surface morphology of the YBCO layer. We will discuss this later.

In order to understand the decrease of J_c of the YBCO(780 °C)/ $Y_2O_3(800\text{ °C})/LAO$ sample in magnetic field, J_c was measured for the set of the samples in which the YBCO layer was deposited at 800 °C and plotted as a function of magnetic field as shown in Fig. 5. Similar to the result observed in the first set, the value and the field dependence of J_c of the $Y_2O_3(800\text{ °C})/YBCO(800\text{ °C})/STO$ sample is almost the same with that of the pure YBCO. The value of J_c of the YBCO(800 °C)/ $Y_2O_3(800\text{ °C})/LAO$ sample, contrary to the previous result, is about 3 times larger than that of the pure YBCO at zero field and this enhancement is maintained in all range of fields.

The opposite behaviors of J_c of $Y_2O_3(800\text{ °C})/YBCO(780\text{ °C})/STO$ and $Y_2O_3(800\text{ °C})/YBCO(800\text{ °C})/STO$ in fields might come from the difference in the surface morphology of the YBCO layer deposited at different temperatures. As shown in Fig. 3 and summarized in Table 1, the YBCO layer deposited at 780 °C has relatively rough surface and many deep holes of which dimensions and density

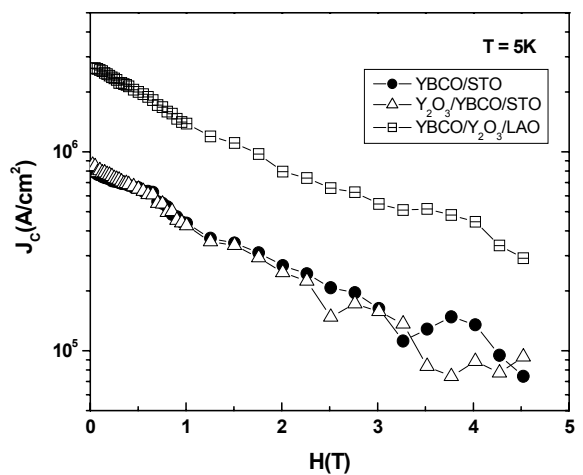


Fig. 5. Comparison of J_c values of YBCO(800 °C)/STO, $Y_2O_3(800\text{ °C})/YBCO(800\text{ °C})/STO$ and YBCO(800 °C)/ $Y_2O_3(800\text{ °C})/LAO$ measured at $T = 5$ K.

are comparable with those of Y_2O_3 nanoparticles. These holes seem to behave as intrinsic pinning centers. Since there exist enough intrinsic pinning centers already, introduction of artificial pinning centers in form of Y_2O_3 nanoparticles leads to reduction in superconducting areas and J_c decreases as the field is increased as shown in Fig. 4. On the other hand, the holes on the YBCO layer deposited at 800 °C are much less and smaller than those on the YBCO layer deposited at 780 °C. This indicates that less numbers of intrinsic pinning centers exist in the set of samples deposited at 800 °C manifested by smaller J_c of the undoped YBCO sample at zero field than that of sample deposited at 780 °C. As artificial pinning centers in the form of Y_2O_3 nanoparticles were added to YBCO films, pinning property is greatly enhanced, and the value and the field dependence of J_c become comparable with those of the pure YBCO deposited at 780 °C.

IV. Summary

Two sets of samples of YBCO thin films with Y_2O_3 nanoparticles were prepared by PLD at different deposition temperatures of YBCO (780 °C and 800 °C) in order to see the change in flux pinning property of the YBCO thin films. The number of laser pulse of 160 was chosen to deposit Y_2O_3 nanoparticles. The existence of textured Y_2O_3 nanoparticles was confirmed by the XRD and AFM analyses. Changes in flux pinning property were probed by evaluating J_c of the two sets of samples from the magnetization measurements. At lower deposition temperature of YBCO of 780 °C, the YBCO layer has rough surface with large density of deep holes which serve as intrinsic pinning centers, so introduction of artificial pinning centers in the form of Y_2O_3 nanoparticles led to reduction in J_c of the YBCO thin films in fields. But the results were different for the YBCO thin films deposited at higher temperature of 800 °C. The smoother film surface contained less amount of intrinsic pinning centers and consequently the addition of Y_2O_3 nanoparticles

effectively enhanced flux pinning property of YBCO leading to increase in J_c .

Acknowledgments

This work was supported by the research grant of the Chungbuk National University in 2009.

References

- [1] T. P. Orlando, K. A. Delin, Foundations of applied superconductivity, Addison-Wesley (1990).
- [2] J. L. Macmanus-Driscoll, S. R. Foltyn, Q. X. Jia, H. Wang, A. Serquis, L. Civale, B. Maiorov, M. E. Hawley, M. P. Maley, D. E. Peterson, Nature materials **3**, 393 (2004).
- [3] T. J. Haugan, P. N. Barnes, T. A. Campbell, A. Goyal, A. Gapud, L. Heatherly, S. Kang, Physica C **425**, 21-26 (2005).
- [4] P. Mele, K. Matsumoto, T. Horide, O. Miura, A. Ichinose, M. Mukaida, Y. Yoshida, S. Horii, Physica C **426-431**, 1108-1112 (2005).
- [5] S. K. Viswanathan, A. A. Gapud, M. Varela, J. T. Abiade, D. K. Christen, S. J. Pennycook, D. Kumar, Thin solid film **515**, 6452-6455 (2007).
- [6] M. Sparing, E. Backen, T. Freudenberg, R. Huhne, B. Rellinghaus, L. Schultz, B. Holzapfel, Supercond. Sci. Technol. **20**, S239-S246 (2007).
- [7] P. Mele, K. Matsumoto, T. Horide, A. Ichinose, M. Mukaida, Y. Yoshida, S. Horii, Physica C **463-465**, 653-656 (2007).
- [8] T. Haugan, P. N. Barnes, I. Maartense, C. B. Cobb, J. Mater. Res. **18**, 11 (2003).
- [9] R.J. Gaboriaud, F. Pailloux, J. Perriere, Applied surface science **186**, 477-482 (2002).
- [10] XCheng, Z. Qi, G. Zhang, H. Zhou, W. Zhang, M. Yin, Physica B **404**, 146-149 (2009).
- [11] T.A. Campbell, T. J. Haugan, I. Maartense, J. Murphy, L. Brunke, P. N. Barnes, Physica C **423**, 1-8 (2005).
- [12] JAlbrecht, S. Leonhardt, H. U. Habermeier, S. Bruck, R. Spolenak, H. Kronmuller, Physica C **404**, 18-21 (2004).